CRITICAL DESIGN FACTORS IN THE DEVELOPMENT OF A HYBRID ELECTRIC ADVANCED LOCOMOTIVE PROPULSION SYSTEM

By:

J.D. Herbst
M.T. Caprio
R.F. Thelen

2004 Vehicular Power and Propulsion Symposium, Paris, France, October 6-8, 2004

PR - 368

Center for Electromechanics
The University of Texas at Austin
PRC, Mail Code R7000
Austin, TX 78712
(512) 471-4496

September 3, 2004

Critical Design Factors in the Development of a Hybrid Electric Advanced Locomotive Propulsion System

John Herbst, Matthew Caprio, Robert Thelen
The University of Texas at Austin
Center for Electromechanics
Austin, Texas
j.herbst@mail.utexas.edu

***Abstract* - Hybrid electric propulsion systems have been applied to a range of vehicles, from compact passenger cars to transit buses and rail vehicles. These systems offer improved performance, increased fuel efficiency and reduced emissions. The University of Texas at Austin Center for Electromechanics (UT-CEM) is developing a hybrid electric propulsion system for high speed non-electric passenger locomotives as part of the Federal Railroad Administration's Next Generation High Speed Rail program. The Advanced Locomotive Propulsion System (ALPS) project, introduced at the Fall VTC-2003 conference, seeks to demonstrate technology for a fossil fueled hybrid-electric locomotive propulsion system capable of operation at speeds up to 150 mph on existing infrastructure with acceleration comparable to current generation electric locomotives. Lightweight, high performance fossil fueled locomotives will facilitate the expansion of high speed passenger rail by providing energy efficiency and trip times comparable to electrified systems without the $3-5M per track mile cost of electrification.**

The key elements employed by the ALPS demonstration are a lightweight gas turbine prime mover directly driving a 2.5 MW 15,000 rpm alternator (turboalternator) to provide the steady state power requirements, along with a 480 MJ, 2 MW, 15,000 rpm flywheel energy storage system to provide supplemental power for acceleration and to recover braking energy.

This paper provides a brief description of the ALPS system, updates progress on fabrication and testing of the major components, and presents the critical design issues and solutions developed by the UT-CEM team to produce power components operating in this power and speed regime.

Keywords: hybrid electric propulsion, energy storage, high-speed generator, flywheel

I. SYSTEM DESCRIPTION

The ALPS propulsion system can be divided into two major modules: the prime power module (consisting of the gas turbine, high speed generator and rectifier) and the energy storage module (consisting of the energy storage flywheel, a high speed induction motor/generator, and a bi-directional power converter). Fig. 1 is a block diagram of the ALPS propulsion system showing the interconnection and power flow between the propulsion system components. The high speed alternator, rectifier, flywheel, motor/generator, and power converter components are currently being developed by UT-CEM under the ALPS program [1].

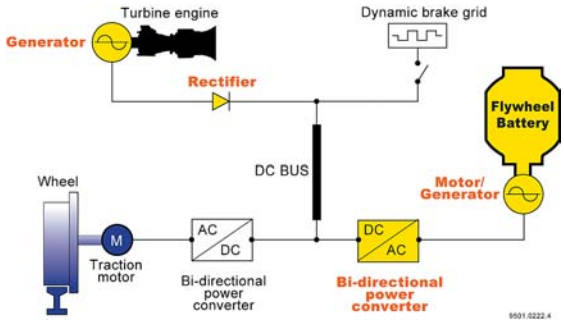

Figure 1. ALPS power flow diagram

Operation of the ALPS prime power module is analogous to the traction drive system in a conventional diesel electric locomotive. To minimize the weight of the propulsion system, the prime power module utilizes a lightweight 15,000 rpm gas turbine in place of the diesel engine. A lightweight, high speed generator is directly coupled to the turbine, eliminating the need for a reduction gearbox, and further reducing the weight of the prime power system. AC power from the high speed generator is fed to the DC bus through a high frequency full bridge diode rectifier. Bi-directional power converters then take power from the DC bus and provide variable frequency AC power to the traction motors mounted on the locomotive trucks. During dynamic (regenerative) braking, the traction motors are driven as generators and feed power back to the DC bus, which can be dissipated in the dynamic brake resistor grids, or in the ALPS system, can be used to recharge the flywheel energy store.

The energy storage module provides supplemental power to the traction drive system during short term power demands such as acceleration or to maintain speed on uphill grades. This allows the locomotive prime power system to be sized to provide only the average power requirements, with the energy storage module providing additional power to meet the transient peak power demands. The ALPS energy storage flywheel,

This material is based upon work supported by Federal Railroad Administration cooperative agreement, DTFR53-99-H-00006 Modification 5, dated April 2004. Any opinions, findings, and conclusions or recommendations expressed in this publication are those of the authors and do not necessarily reflect the view of the Federal Railroad Administration and/or U.S. DOT.

motor/generator and power converter are designed to provide 2 MW of supplemental power for up to three minutes. The energy storage module also allows the ALPS system to recover a significant portion of the kinetic energy in the train, taking energy normally dissipated as heat in the dynamic brake resistor grids and using it to reaccelerate the flywheel. This energy is then available to the locomotive traction system during the next power demand cycle. The energy storage system is also used to provide load leveling for the gas turbine by managing rapid changes in traction power demand. This allows the turbine to operate at steady power levels for longer durations, minimizing the number of thermal transients and greatly extending the maintenance intervals on the engine.

The sections below provide brief descriptions and discuss some of the critical design issues of the high speed generator, energy storage flywheel, motor/generator, and power converter, four of the critical components of the propulsion system.

II. HIGH SPEED GENERATOR

The 15,000 rpm 2.5 MW continuous duty ALPS generator is an eight pole, 3 phase synchronous machine approximately 0.7 m diameter X 1.37 m long weighing approximately 1,100 kg. Development of the high speed generator was initially conducted in conjunction with Honeywell, although they are no longer participating in the development efforts. Fig. 2 is the ALPS generator during initial no-load testing at UT-CEM.

The generator features a brushless exciter and rotating diode array to provide excitation current to the field windings. The rotor is a salient pole design supported on conventional oil jet lubricated rolling element bearings mounted in squeeze film dampers. High performance carbon seals are used to isolate the rotor cavity from bearing lubrication and cooling oil.

A. Rotor Laminated Core

In order to manage stresses created by the high rotational speed, the rotor core is constructed of heat treated 4130 alloy steel laminations. The interference fit assembly of the rotor laminations to the shaft was a critical issue in the design of the high speed generator. Due to high operating stresses and stress concentrations caused by keyways, it is not possible to lock the core to the shaft using conventional techniques. Therefore, the core/shaft interference fit must retain adequate radial compression at 15,000 rpm to transmit operating and transient torques with adequate margins. The low inertia of the high speed generator and turbine prime mover also pose a risk of transient overspeeds; the core/shaft fit must maintain contact under this condition to avoid severe imbalance loads. These conditions dictated a diametrical interference of 0.635 mm on a 135 mm diameter shaft, which results in a 207 MPa (30 kpsi) interface pressure at rest. The high assembly interference and interface pressure greatly complicate the core assembly process and raise the risk of conical buckling of the laminations.

Although not widely reported in the literature, conical buckling of high interference fit laminated rotor core assemblies has occurred in prototype machine designs, including one at our research laboratory. Buckling of the laminations will relieve interface pressure and results in unacceptable deflections of the core structure. For the ALPS rotor, a novel design methodology was devised to predict and prevent conical buckling of the core through structural design [2]. This approach depends on the axial deflection stiffness of specifically designed features of the rotor structure to contain the buckling motion.

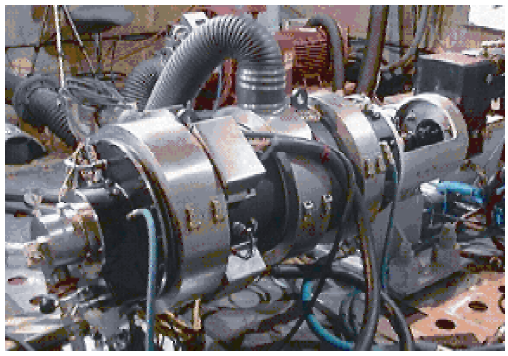

Figure 2. ALPS generator during no-load testing.

The buckling prevention analysis consists of approximating the force-deflection characteristics of individual buckled laminations, and applying those forces to a finite element model of the structure to quantify the resulting deflection. A buckling force-displacement curve was generated based on closed form predictions for a single lamination, and is shown in Fig. 3.

As the predicted axial forces generated by the buckling lamination increase to a peak value with increasing displacement and then roll off, a peak buckling force can be estimated, and its respective deflection level is defined as the "critical buckling deflection." The peak load is then applied to the structural model, and the resulting deflection is calculated. The analysis criterion assumes that if the axial displacement of the rotor structure is equal to or greater than the critical buckling deflection, the core will conically buckle. If however the resulting displacement is substantially less than the critical buckling deflection, the assembly is presumed to be structurally stable, with only negligible amounts of conical deformation of the core. This approach was successfully used to design the high speed generator end turn supports and clamp rings, which make up the axial support structure for the core. The core assembly procedure was also designed to ensure adequate structural support of the core.

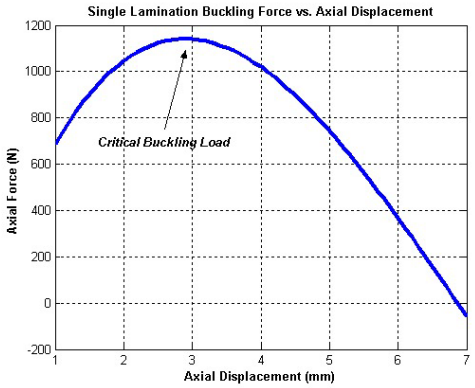

Figure 3. Predicted force of buckling lamination

The high interference and constraints on the allowable component temperatures limited the diametrical assembly clearance to only 0.127 mm. The shaft was cooled with liquid nitrogen and the core assembly and clamp structures were heated with flexible ceramic band heaters. In order to offset the axial growth of the shaft and contraction of the core during the temperature equalization process, axial compression must be maintained on the core for the support structure design to be effective. A custom hydraulic clamping cylinder with the clamp load reacted directly to the shaft was used to maintain axial compression of the core throughout the temperature equilibration process. The annular cylinder provided access to a clamp nut on the shaft, which was periodically tightened to maintain axial compression once the hydraulic clamp load was removed. Fig. 4 shows the core assembly and shaft prior to the fit along with a picture after successful installation of the core. Note the dual taper shaft starter and annular clamping cylinder visible in the pictures.

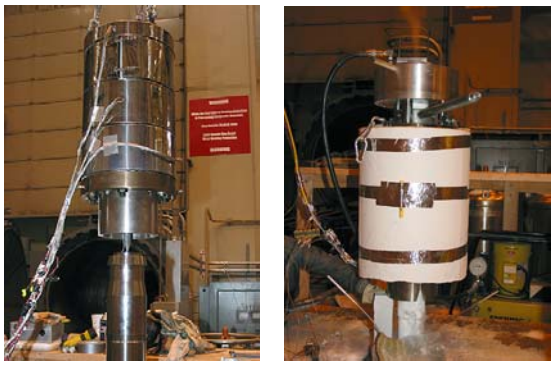

Figure 4. Core/shaft components before and after assembly.

B. Field Winding and Cooling

Once the core and end turn supports were assembled on the shaft, the eight series connected field coils were installed. The field windings are constructed of 0.81 mm x 11.43 mm rectangular copper strip edge wound to form a flat racetrack coil. High centrifugal loads associated with 15,000 rpm operation prevented the use of conventional techniques for securing the pole heads over the field windings. As shown in Fig. 5, the high strength 4130 laminations incorporate an integral pole head, requiring the field coils to be wound in place.

Figure 5. Field winding and cutaway of oil cooling wedge.

Several design issues were identified during initial testing of the high speed generator. These design issues have been addressed and final assembly of the generator is nearing completion. After no-load testing at the UT-CEM lab, the generator will be moved to the Naval Business Center in Philadelphia for load testing. After load testing, the generator will be returned to UT-CEM for integration with a Pratt & Whitney gas turbine for further laboratory and locomotive demonstration testing.

The compact design and high rotational speed of the generator make thermal management extremely challenging; cooling for the machine is accomplished with a combination of air and oil cooling. Fig. 5 also shows a cutaway of a Honeywell patented integral oil cooling wedge with the 4-pass internal oil cooling passages revealed [3]. The cooling oil is routed through annular passages in the shaft to provide cooling for the bore of the laminated core assembly before being routed through radial ports to the oil cooling wedges. The rotor oil cooling system is supplemented with forced air cooling of the field coil end turns and rotor/stator air gap.

III. ENERGY STORAGE FLYWHEEL

The ALPS flywheel utilizes a high strength graphite composite material for the main body of the rotor, providing a safe, robust, compact unit suitable for use in a mobile environment [4]. The flywheel is oriented vertically in a two axis gimbal mount to minimize gyroscopic loads on the bearings and chassis. The 480 MJ (130 kWh) energy storage flywheel is designed to operate between 7,500 and 15,000 rpm, delivering and receiving up to 360 MJ from the locomotive traction system [5]. The main components of the flywheel are the composite rotor, the magnetic bearing system, the touch down bearing system, the composite liner, the vacuum penetration shaft seal, and the containment housing. The flywheel can be seen during spin testing in Fig. 6.

Critical issues for the flywheel include fabrication and assembly of the rotor composite structure, magnetic bearing rotor materials, rotor dynamics, and the shaft vacuum penetration.

Figure 6. ALPS Flywheel undergoing spin testing.

A. Composite Rotor Flywheel Design

For a compact, lightweight, mobile-application flywheel design, energy density must be maximized by taking advantage of the speed squared relationship of stored kinetic energy, and operating at as high a speed possible for a given geometry (even if doing so requires lighter materials). As composite wheels can operate at tip speeds in the range of 1000 m/s while steel can only withstand approximately 300 m/s, composite materials are used for high performance flywheels. The winding of engineered composite materials and design of a prestressed nested ring flywheel body are thus critical design factors for the rotor of the high speed ALPS flywheel. Composite rotor design and fabrication, while technically challenging, has become a routine core competence of UT-CEM as many successful rotors have been constructed in this manner. For further information on UT-CEM's approach to winding design, analysis, and testing, please refer to [6,7].

The flywheel rotor was designed to be constructed of 15 nested rings, interference fit together on tapered surfaces to maintain compressive preload at each interface throughout the speed range. This design approach results in robust safety characteristics by preventing possibility of a cascade failure.

The structure of each ring (including the number and size of graphite winding increments, filament tension, winding angle, fiber volume, epoxy content, and cure cycle profile) were analyzed, then carefully controlled and inspected during fabrication. Hydroburst testing was used to verify that delivered mechanical properties were achieved.

Assembly interference of the rings was optimized with nested ring and axisymmetric analyses. Selecting the fits to achieve minimum stress in each ring and adequate interface pressure at speed required multivariable optimization. During installation, strain data is recorded to allow for adjustments in subsequent fits to accommodate for difference between designed and achieved interferences.

The axial press load of the interference fit rings becomes a critical design factor on the outermost rings as the axial force increases with the diameter of ring installed. In order to minimize press load and prevent axial compression failure of the ring during installation, the interface surface is lubricated by a combination of a wound layer of Randolite™ and a wet epoxy coating. Further, outer rings are split in half lengths to reduce the required press load.

A composite containment burst liner was incorporated into the flywheel housing design to absorb the energy of the burst of the outer flywheel ring. The outer ring was designed to be the most highly stressed ring so that it would burst first in the event of overload or material degradation, thus controlling and limiting the burst energy for the liner design. Dynamic simulations were performed by Argonne National Lab to predict the performance of the containment liner [8].

B. Magnetic Bearing Rotor Materials

The flywheel rotor is supported by non-contacting magnetic bearings to provide for a long operating life at high speed. Conventional rolling element bearings are not a reasonable option in this application due to their limited operating life at this combination of speed and diameter (1,350,000 dN), and due to the difficulty of supplying adequate continuous lubrication and cooling in the vacuum environment. Grease lubricated ball bearings are used however as "backup bearings" which can catch and support the rotor temporarily in the event of a magnetic bearing system fault.

The active magnetic bearing system supports the rotor in five axes: vertical thrust, and two orthogonal radial axes ('X-Y') at both ends of the rotor [9]. The rotor components of the radial magnetic bearings are constructed of steel alloy laminations with an insulating coating to suppress eddy current losses as the magnetic field essentially varies at frequencies up to 250 Hz (maximum rotational speed). At the operating speed, temperature, and required magnetic field strength of this application, the combination of magnetic and mechanical material properties becomes a critical design factor for the flywheel.

High stresses are generated in the laminations due to two sources: the interference fit required to maintain attachment to the shaft at speed, and the centrifugal loading of the laminations while at speed. Under extreme operating conditions, this combined stress on the radial bearing rotor laminations can reach 338 MPa (49 kpsi). Few grades of magnetically soft "electrical steel" can tolerate this level of stress.

The application of this flywheel is not particularly sensitive to parasitic losses in general as it is employed in a power averaging mode rather than long-term energy storage. However, hysteresis losses in the radial bearing laminations are critical as the rotor is only passively cooled through radiation. Losses on the rotor give rise to heat which must be rejected across the vacuum to the actively cooled magnetic bearing stators. In this way, the core loss of the rotor lamination material has a role in dictating the steady state operating temperature of the lamination stacks. The temperature of the rotor laminations should be kept below 175°C (350°F) to limit the thermal growth of the rotor, as rotor growth acts to reduce the air gap of the magnetic bearing, increasing the effective negative stiffness of the bearing, and influencing dynamic control stability.

The rotor lamination material selection therefore constitutes a compromise between low magnetic loss properties and high mechanical strength. Available materials were compared based on their combination of core losses and mechanical strength for suitability to this application. During our search, the field was limited to three compositions meeting the minimum strength requirements: M19 (the highest strength non-oriented electrical steel grade), Hiperco™ Alloy 50 (49%Co, 2%V, Balance Fe), and 4130 high strength alloy steel. Although the materials are to be used in a variable frequency magnetic environment, loss values were compared at 60 Hz where they are conventionally measured. The results are summarized in Table I.

While Hiperco appears to have the best combination of low losses and high mechanical strength, it was eliminated as an option for these laminations as it was only available in sheet widths up to 250 mm (10"), and these bearings must be 280 mm (11") in diameter to provide adequate force. Annealed 4130 steel was therefore initially chosen to provide significant safety margin for the first prototype.

TABLE I. OPTIONS FOR RADIAL BEARING LAMINATION MATERIALS

Lamination Material 29 Gauge 0.35 mm / (0.014")	***Test Induction @ 60 Hz***	***Hysteresis core loss (W/kg)***	***Mechanical Yield Strength MPa / (kpsi)***	***Mechanical Ultimate Stength MPa / (kpsi)***	***Elong -ation (%)***
M19	15 kG	3.3	367 / (53.2)	503 / (73)	21
Hiperco 50 cold rolled	--	--	1275 / (185)	1345 / (195)	1
Hiperco 50 heat treated	15 kG	4.8	483 / (70)	861 / (125)	9
4130 Steel annealled	11 kG	~8.9	538 / (78)	758 (110)	28
4130 Steel heat treated	--	--	1358 / (197)	1613 / (234)	12

Unfortunately, the first phase of flywheel testing [10] revealed that the scaled loss predictions, based on 60 Hz loss data for 4130, significantly underpredicted actual losses in the radial bearing rotors, resulting in excessive heating on the rotor. At the present time a design change is under consideration to replace the laminations with M19 material to extend run time.

Detailed analysis and hysteresis loss testing of lamination materials is underway at UT-CEM at the representative frequencies and field strengths in order to further improve prediction of radial magnetic bearing losses. Additionally, it should be noted that the material compromise critical design factor can be largely eliminated in a next generation rotor through active cooling. With active cooling of the rotor, higher core losses can be tolerated while utilizing high strength steel alloys for larger factors of safety against yield, and infinite fatigue life.

C. Rotordynamic Performance

Stability and control of the high speed rotor of a large energy storage flywheel is nontrivial, especially if energy density goals are aggressive. Critical rotordynamic factors include the design of the rotor, the active magnetic bearing compensator design, and the performance of the backup bearing system.

The challenge in designing the flywheel rotor involves selecting the appropriate mass and stiffness ratios so that the resulting flexible modes of the rotor occur at frequencies above the maximum operating speed. Additionally, the rotor is "gyroscopic", meaning that the flexible modes change with operating speed. To further complicate the design decisions, the fact that the rotor is supported by active magnetic bearings implies that the dynamics of the magnetic bearing actuators and the control system strongly influence the rotor response.

The interdependent factors of rotor structure and control dictate that design, analysis, and simulation be an iterative process. Solid modeling, finite element structural analysis, modal analysis, control law simulations, and electrical circuit design are performed in parallel, on a system of evolving parameters, to optimize the design for realistic physical limits, while meeting the design goals. Through this intense and complex process, numerous critical design parameters such as rotor shaft stiffness, radial bearing air gap, radial bearing coil configuration, bearing power amplifier rating, and control compensator gains were jointly determined. In this way, the rotordynamic design and synthesis method itself becomes a critical design factor.

Given the significant amount of energy stored in the ALPS flywheel, a robust backup bearing system is essential to provide for a safe, controlled shut down in the event of a failure of the magnetic bearing system. Through the course of flywheel and rotor technology development history, some units have failed catastrophically after a loss of magnetic bearing control due to unstable behavior while supported on backup bearings [11]. The design, analysis, and testing of the performance of the backup bearing performance was a critical safety issue for the high energy ALPS flywheel.

Design and selection of appropriate backup bearings is the first step in controlling the performance of the rotor during magnetic bearing fault. The bearings and support structure have been selected to provide relatively low frequency rigid body modes. Additionally, squeeze film dampers were incorporated in the backup bearing support system to reduce the response due to a transient drop onto the backup bearings.

"Drop test" experiments were also performed to ensure that the behavior on the backup bearings was satisfactory. To further improve the performance of the rotor on backup bearings, a novel semi-passive "whirl arresting" circuit was developed to effectively lock the rotor into a specific quadrant if undesirable whirl occurs [10]. This feature emulates the gravity field potential energy well that prevents whirl in many horizontal rotors.

D. Shaft Penetration Design

An evacuated housing is common practice in flywheel designs to reduce the aerodynamic surface heating of the high speed rotor. Often, flywheels utilize a topology in which the motor generator operates within the vacuum, eliminating the need for rotating vacuum seals. For the ALPS flywheel, the 2 MW power level and active duty cycle dictate that the motor generator be outside the vacuum to isolate motor/generator heat loads from the flywheel rotor.

The flywheel rotor shaft must exit the vacuum enclosure and couple to the motor generator, thus requiring a rotating seal. The shaft vacuum penetration presents numerous design complexities, including seal selection, seal support, and coupling of the flywheel to the motor generator. The connection must also manage the cyclic torque loads and misalignment of the flywheel and motor/generator shaft. To minimize the axial length of the system, the shaft vacuum seal has been integrated onto the center shaft of a conventional flexible disk coupling. The detailed components of the penetration area of the flywheel can be seen in Fig. 7.

Numerous seal approaches were considered for this demanding 1 mTorr, 15,000 rpm shaft application. Ultimately, successful bench testing led to the selection of a FerroTec™ magnetic fluid filled labyrinth type seal for the shaft penetration. This seal relies on multiple stages of labyrinth passages filled with magnetic fluid, held in place by strong permanent magnets to resist the spin loads and vacuum force. Seal drag and the internal seal bearings generate heat, therefore the seal is actively liquid cooled.

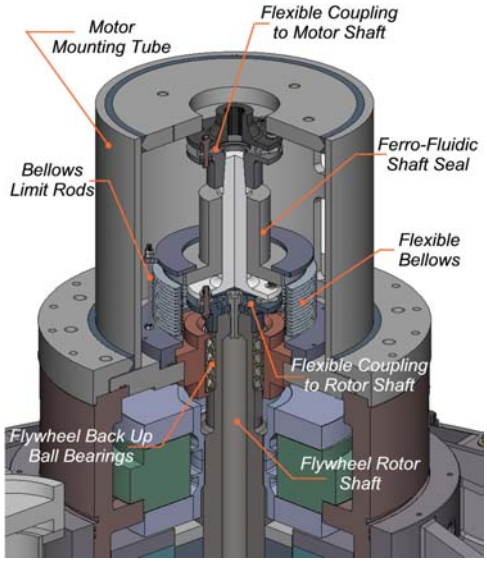

Figure 7. Flywheel shaft penetration components.

Due to the movement of the flywheel rotor within the magnetic bearing control space (+/- 0.5mm radial, +/- 0.25 mm axial), the seal must be able to accommodate the offset misalignment that can develop between the flywheel rotor and the motor generator shaft. For this reason, the seal housing must be compliantly mounted to the flywheel housing through a flexible bellows, with a set of flexible couplings on each side of the seal through shaft. The through shaft diameter must be sized to the minimum required for torque transmission so that the surface speed and shear forces experienced by the ferrofluid are within acceptable limits.

The flexible bellows and coupling arrangement is a complicating factor in that it adds dynamics to the rotating assembly which must be adequately damped, requires precise alignment for smooth operation, and results in low torsional stiffness between the flywheel and motor generator.

IV. MOTOR/GENERATOR AND POWER CONVERTER

The flywheel is connected to the locomotive DC bus with a 15,000 rpm induction motor/generator and high frequency soft-switching power converter. The induction machine is a conventional squirrel cage design wound in a three phase, two pole configuration to minimize the electrical operating frequency at high speed. The rotor is constructed with high strength alloy steel laminations and beryllium copper endrings to manage the high operating stresses. The rotor is supported on conventional oil cooled rolling element bearings mounted in oil filled squeeze film dampers. Critical issues for the motor/generator include processing and assembly of the rotor laminations and end rings, strength and reliability of the bar to end ring braze connections, thermal management in a high power density machine, and torsional coupling harmonics.

A. Rotor Materials Selection

The flywheel induction motor-generator rotor, operating at 15,000 rpm with a tip speed of 286 m/s, shares the demanding lamination requirements with the high-speed turbine driven generator described in an earlier section. The motor generator core utilizes heat treated 4130 steel laminations to manage spin stresses and large interference fit to maintain contact pressure at speed. Interference fit design and analysis to prevent conical buckling of this core was performed in a similar manner to the process described for the high speed generator.

As an additional critical design factor specific to the induction motor, end rings must be mounted to the shaft and maintain integrity at speed and high temperatures. Designing an end ring for high speed operation is more demanding than a magnetic core, as the end ring material has the additional requirement of having low electrical resistance. High conductivity aluminum and copper alloys were considered for the end ring, but ultimately only Beryllium Copper alloys were able to meet the strength and conductivity requirements of the application. BeCu Alloy 3 was selected with 63% IACS electrical conductivity and 669 MPa (97 kpsi) yield strength. For the bars, Zirconium Copper Alloy C15000 was selected with 90% IACS conductivity and 455 MPa (66 kpsi) ultimate strength.

It is common in squirrel cage induction motor designs for the end ring to be supported by the rotor bars, either as an integral casting, or through brazed joints. However, at these tip speeds, the ring must be positively piloted to the shaft to ensure stable balance properties. The end ring was therefore designed with an interference fit to the shaft which maintains radial contact pressure under all speed and temperature conditions. This design criterion implies a large interference as the end ring grows significantly due to spin loads and thermal growth as copper alloys have relatively high mass densities and coefficients of thermal expansion. Additionally, a non-uniform end ring section was utilized to reduce the mechanical load on the component with minimal impact on electrical properties.

B. End Ring Joint Design

The electrical and mechanical joint between the rotor conductor bars and end rings is a critical area of the flywheel motor which required significant design, analysis, and testing. Numerous unique features were incorporated into the design of this region of the machine in order to reduce the stresses of the bar-end ring joint, as shown in Fig.8.

Speed and thermal growth of the end ring is larger than that of the lamination core, and as the bars connect these components, significant stress is generated in this joint area. A spacer was added between these components to provide a region over which the shear at this interface could be translated to more benign bending. Additionally, a boss feature was incorporated into the end ring to blend the strain of the bar and alleviate the stress concentration at the joint [2].

Substantial efforts were dedicated to selecting and testing a high strength, low process temperature solder suitable to make the final connection between the end rings and the bars. Ultimately, 80Au 20Sn solder was chosen, demonstrating approximately 140 MPa (20 kpsi) shear strength, 275 MPa (40 kpsi) tensile strength, with a process temperature of 300°C (575°F). Fig. 9 shows tensile sample tests, single lap shear specimen tests, representative geometry samples, induction heating processing, and metallurgical joint layer inspection that were carried out in support of this joint design.

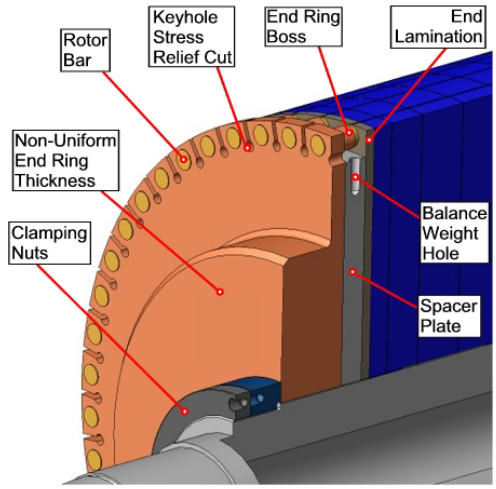

Figure 8. Key features of motor end ring joint design.

C. *Motor Thermal Management*

Compact, power dense machines such as the flywheel induction motor are typically demanding applications for thermal management as the volume and surface area (critical factors for heat transfer) are minimized. At the 2 MW motor rating, approximately 65-85kW of losses (depending on operating conditions) must be removed.

The stator cooling system relies on a combination of oil jackets on the stator and forced air over the end turns and down the air gap, exiting radially at the midplane of the machine. The common forced air circuit is the only mode of cooling for the rotor. In order to maintain a rotor core operating temperature less than 175°C (345°F), an air flow rate of 57 standard cubic meters per minute (2000 SCFM) was required.

D. *Torsional Coupling Harmonics*

Electrical circuit simulations showed that interaction between the motor drive switching harmonics and the motor results in significant fluctuating torques (0.10-0.15 pu) at relatively high frequencies (8400 Hz), suggesting that torsional fatigue of the coupling system could be an issue.

The transmissibility of the mechanical system of the motor, shaft, and coupling was analyzed to determine if the predicted harmonic torques would cause fatigue damage. The results showed that the inertia of the motor would absorb the high frequency torque ripple, and essentially isolate the coupling system from the harmonics. The transmissibility of the system as a function of frequency can be seen in Fig. 10.

While the high frequency ripple torque generated by motor-drive interaction ultimately was not an issue in coupling fatigue life, it nevertheless indicated that the individual bars will experience significant force fluctuations, and should be adequately restrained to prevent joint fatigue fracture. To this end, the clearance between core slots and rotor bars will be filled with thermally stable epoxy through vacuum impregnation after assembly.

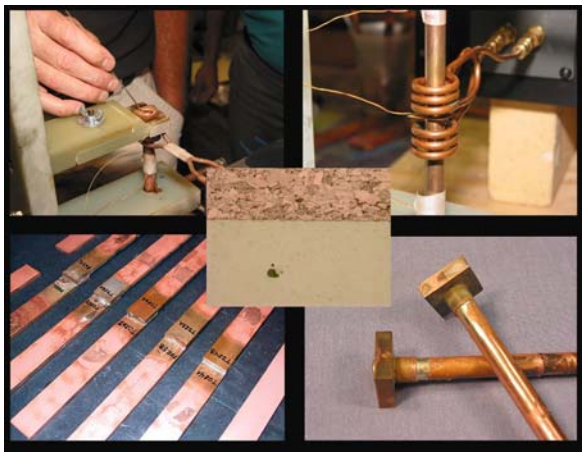

Figure 9. Solder joint processing development and testing.

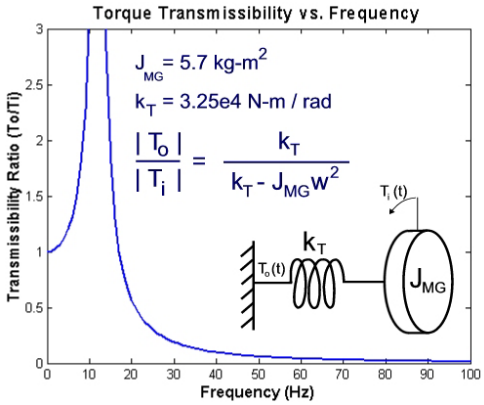

Figure 10. Motor ripple torque attenuation.

E. *Power Converter*

A two-pole motor design was selected to limit power frequencies to 250 Hz. The high speed motor design results in a compact motor construction for the given design rating of 2 MW-continuous, and makes a positive contribution towards the overall size and mass of the flywheel system. The same compactness, however, affects the thermal management challenge, reinforcing the need to lower losses in the motor. A low-slip, high-efficiency induction machine design was completed, and the motor drive was then designed to minimize its contribution of harmonic losses in the motor. The drive amplitude modulation ratio (m_a) is kept below 1.0 for a non-clipped, sinusoidal average voltage to the motor. Since the dc-link voltage was given at 1960 V[dc] by prior locomotive design, the flywheel motor was designed to a base voltage of 1100 V[rms]. Secondly, the frequency modulation ratio (m_f) was kept high (> 15) by employing a soft-switching scheme. Switching frequency is generally limited by the losses that can be accommodated by switch selection and cooling methods. Soft-switching reduces losses by controlling the switch closing and opening to occur at zero voltage or current conditions [12]. Using an auxiliary resonant commutated pole (ARCP) design [13], the projected switching frequency limit was raised to 4 kHz. Fig. 11 shows the basic switch topology for ARCP. The quasi-resonant switching is designed for a 40 kHz resonance.

An area of interest for the design and modeling of the drive is to check the variance of the resonant component values under different conditions. For example, the value of the auxiliary switched inductors was found to change by -11% over the 60 Hz to 40 kHz frequency range, the latter being the domain of interest for the resonant switching event. Some variances can also be expected in the inductor values over the full current range and the resonant capacitors over the full voltage range. Beyond these, changes are known to occur with temperature and aging. These parameter values will be used in simulation models to bracket the range of resonant switching performance and design the timing sequence accordingly.

Each switch location in the bridge is served by six IGBT assemblies, three parallel paths of two in series. The auxiliary leg switches and individual inductors are arranged with three assemblies operated in parallel. During tests, the voltage and current sharing in each combination assembly will be checked against design tolerances. Fig. 12 shows the assembled inverter electronics package during early testing. At this writing, the power converter has been assembled and partially tested. Some setbacks in early testing have led to further analysis and testing of the system logic and circuits. The project goal is to have the inverter ready for operation in 1st quarter 2005.

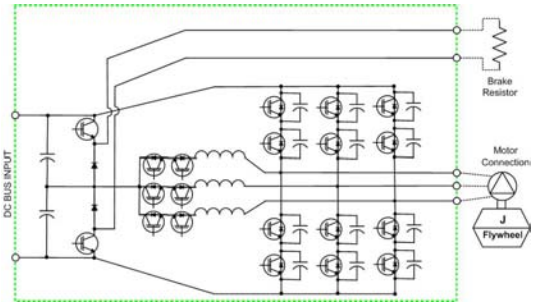

Figure 11. Schematic of ALPS ARCP inverter topology

Figure 12. ALPS flywheel electronic drive during early tests

V. SUMMARY

The ALPS project is advancing the state-of-the-art in critical power generation, energy conversion and energy storage technologies to demonstrate an advanced hybrid electric propulsion system for high speed passenger locomotives. Significant advances include: processing and assembly of laminated cores for high speed machines, design and assembly of composite flywheel rotors and containment systems, control of rotor whirl in active magnetic bearings, flexible couplings with integrated high speed vacuum shaft seals, design and manufacture of novel high speed induction machines, thermal management of high power density machines using combined air/oil cooling, and high power ARCP soft switching power converters.

Some initial component testing has been completed and fabrication of the prototype electric machines and energy storage flywheel is nearing completion. After laboratory testing of the assembled system in 2005, the system will be integrated onto locomotive chassis' for rolling demonstrations at the Transportation Technology Center's high speed test track in Pueblo Colorado in 2006.

REFERENCES

[1] J.D.Herbst, M.T.Caprio, and R.F. Thelen, "Advanced Locomotive Propulsion System (ALPS) Project Status 2003", 2003 ASME International Mechanical Engineering Congress and Exposition, November 15-21, 2003, Washington, DC.

[2] M. Caprio, V. Lelos, and J. Herbst, "Design and Stress Analysis of a High Speed Rotor for an Advanced Induction Machine," Electric Machines Technology Symposium, Philadelphia, PA, January 27-29, 2004.

[3] US Patent # 6,113,624, "Winding wedge retention to maintain coil form."

[4] R.F. Thelen, J.D. Herbst, and M.T. Caprio, "A 2 MW Flywheel for Hybrid Locomotive Power", IEEE Semiannual Vehicular Technology Conference VTC2003-Fall, October 6-9, 2003, Orlando, FL.

[5] M.T. Caprio, R.F. Thelen, J.D. Herbst, 2 MW 130 kWh Flywheel energy storage system, Electrical Energy Storage - Applications and Technology (EESAT2003), October 27-29, 2003, San Francisco, CA.

[6] R.J. Hayes, J.P. Kajs, R.C. Thompson, J.H. Beno, "Design and testing of a flywheel battery for a transit bus," 1999 SAE International Congress and Exposition, March 1999, Detroit, Michigan.

[7] R.C. Thompson, T.T. Pak, B.M. Rech, "Hydroburst test methodology for evaluation of composite structures," ASTM 14th Symposium on Composite Materials: Testing and Design, Special Technical Publication 1436, Paper ID 10877, March 2002, Pittsburgh, Pennsylvania.

[8] B.J. Hsieh, R.F. Kulak, J.H. Price, B.T. Murphy, "Transient analysis of a flywheel battery containment during a full rotor burst event," ASME Pressure Vessels an Piping Division, v370, 1998, Finite Element Applications: Linear, Non-Linear, Optimization and Fatigue and Fracture, Proceedings of the 1998 ASME/JSME Joint Pressure Vessels an Piping Conference, July 1998, San Diego, CA, p 101-106.

[9] B.T. Murphy, H. Ouroua, M.T. Caprio, J.D. Herbst, "Permanent magnet bias homopolar magnetic bearings for a 130 kW-hr composite flywheel," International Symposium on Magnetic Bearings 9, August 3-6, 2004, Lexington, KY.

[10] M.T. Caprio, B.T. Murphy, J.D. Herbst, Spin commissioning and drop tests of a 130 kW-hr composite flywheel, International Symposium on Magnetic Bearings 9, August 3-6, 2004.

[11] A.R. Bartha, "Dry friction backward whirl of rotors: Theory, experiments, results, and recommendations," International Symposium on Magnetic Bearings 2000.

[12] M.D. Bellar, T.S. Wu, A. Tchamdjou, J. Mahdavi, M. Ehsani, "A review of soft-switched DC-AC converters", IEEE Transactions on Industry Applications, vol. 34 number 4 , July-Aug. 1998, pp 847 – 860.

[13] R. W. De Doncker and J. P. Lyons, "The Auxiliary Resonant Commutated Pole Converter," IEEE-IAS Conf. Rec., pp. 1228-1235, 1990.